Structural Engineering and Mechanics, *Vol. 72, No. 6 (2019) 713-722*
DOI: https://doi.org/10.12989/sem.2019.72.6.713

A 3D RVE model with periodic boundary conditions to estimate mechanical properties of composites

Fathollah Taheri-Behrooz* and Emad Pourahmadi[a]

School of Mechanical Engineering, Iran University of Science and Technology, P.O.B. 1684613114 Tehran, Iran

(Received May 10, 2019, Revised July 27, 2019, Accepted August 3, 2019)

Abstract. Micromechanics is a technique for the analysis of composites or heterogeneous materials which focuses on the components of the intended structure. Each one of the components can exhibit isotropic behavior, but the microstructure characteristics of the heterogeneous material result in the anisotropic behavior of the structure. In this research, the general mechanical properties of a 3D anisotropic and heterogeneous Representative Volume Element (RVE), have been determined by applying periodic boundary conditions (PBCs), using the Asymptotic Homogenization Theory (AHT) and strain energy. In order to use the homogenization theory and apply the periodic boundary conditions, the ABAQUS scripting interface (ASI) has been used along with the Python programming language. The results have been compared with those of the Homogeneous Boundary Conditions method, which leads to an overestimation of the effective mechanical properties. According to the results, applying homogenous boundary conditions results in a 33% and 13% increase in the shear moduli G_{23} and G_{12}, respectively. In polymeric composites, the fibers have linear and brittle behavior, while the resin exhibits a non-linear behavior. Therefore, the nonlinear effects of resin on the mechanical properties of the composite material is studied using a user-defined subroutine in Fortran (USDFLD). The non-linear shear stress-strain behavior of unidirectional composite laminates has been obtained. Results indicate that at arbitrary constant stress as 80 MPa in-plane shear modulus, G_{12}, experienced a 47%, 41% and 31% reduction at the fiber volume fraction of 30%, 50% and 70%, compared to the linear assumption. The results of this study are in good agreement with the analytical and experimental results available in the literature

Keywords: Periodic boundary conditions; Asymptotic homogenization theory; Three-dimensional RVE; Mechanical properties; Python scripting; Non-linear resin behavior; USDFLD subroutine

1. Introduction

Due to their high strength and specific stiffness, fatigue strength and better corrosion resistance than conventional materials, composites have become an essential engineering material. They are used in various areas such as aerospace structures and sports, electronic, medical and construction equipment. Therefore, the estimation of their mechanical properties has been one of the important fields of research in recent decades. In addition to experimental methods which are time-consuming and often expensive, micro-macro mechanical methods can be used to estimate the properties of these materials.

In the micromechanical methods, the properties of the composite materials are obtained by an RVE or RUC analysis from the known properties of their components (fiber and resin) (Aboudi 2013). In the macromechanical approach, homogenous structures with anisotropic properties have been substituted with heterogeneous composite structures (Nemat-Nasser and Hori 2013). The advantage of the micromechanical method lies in the fact that not only the general properties of the composite materials can be obtained, but also various mechanisms such as the initiation and growth of failure can be studied (Xia, Chen *et al*. 2000, Ellyin, Xia *et al*. 2002). There are multiple micromechanical methods to analyze and estimate the mechanical behavior of composite materials. The upper and lower limit of the modulus of elasticity has been obtained by the principle of energy variation, and analytical solutions have been utilized (Hashin and Shtrikman 1963, Hashin and Rosen 1964). According to the energy balance approach, with the help of the theory of elasticity, Whitney and Riley (Riley and Whitney 1966) presented an analytical method for the modulus of elasticity of composite materials. Unfortunately, the extension of this method to viscoelastic, elastoplastic and nonlinear composite materials is very difficult. Aboudi (Aboudi 2013) extended the unified micromechanical approach based on the study of the interactions of periodic cells and used it to predict the general behavior of composite materials and inelastic structures. He utilized homogenous boundary conditions applied to an RVE or the unit cell models which are only applicable for cases where normal traction is applied on the boundaries. For shear loading, many researchers including Needleman and Tvergaard (1993), Sun and vaidya (1996) and Suquet (1987) proved that the 'plane-remains-plane' boundary conditions are of the over-constrained type.

The micromechanical methods mentioned above can be considered as mechanical or engineering models. Mathematical models emerged in 1970s with the

*Corresponding author, Associate Professor
E-mail: taheri@iust.ac.ir
[a] M.Sc. Student

http://www.techno-press.com/journals/sem&subpage=7
ISSN: 1225-4568 (Print), 1598-6217 (Online)

generalization of the Asymptotic Homogenization Theory (AHT), opposing the engineering methods. The basis of this theory lies in the works of Suquet (1987), Benssousan (Bensoussan, Lions *et al*. 2011), Sanchez-Palencia (1980) and Bakhvalov and Panasenko (1984). The homogenization theory uses periodic boundary conditions explicitly in the linear and nonlinear modeling of composite materials (Tchalla, Belouettar *et al*. 2013). These results indicate that some specific kinds of deformation do not result in a change in planar boundaries after deformation (Suquet 1987). Guedes and Kikuchi (1990) examined composite problems regarding the subject of the application of finite element method based on the theory of asymptotic homogenization. The application of the asymptotic homogenization theory has been used in various cases of composite materials analysis by Raghavan (Raghavan, Moorthy *et al*. 2001), Moorthy and Ghosh (1998).

Hori and Nemat-Naser (1999) showed that the predicted effective modulus of elasticity could vary according to the conditions applied at the boundaries of the unit cell where the boundary conditions of homogeneous displacement and homogeneous traction will yield the upper and lower limits of the modulus of elasticity. Hollister and Kikuchi (1992) presented a good comparison between the asymptotic homogenization theory and mechanical methods (named the Average Field Theory in the study of Hori and Nemat-Naser (1999)) and concluded that the asymptotic homogenization theory, which uses periodic boundary conditions, yields much more accurate results. It was also proved that the asymptotic homogenization theory and the mechanical methods could be correlated, resulting in a useful hybrid theory.

The finite element method has been extensively used for the analysis of the periodic unit cell with the goal of determining the mechanical properties and the failure mechanisms of composite materials (Adams and Crane 1984, Pindera and Aboudi 1988, Aboudi 1990, Allen and Boyd 1993, Bonora, Costanzi *et al*. 1994, Chu, Yu *et al*. 2015, Ma, Wriggers *et al*. 2016, Belkacem, Tahar *et al*. 2018, Liao, Tan *et al*. 2018, Yahia, Amar *et al*. 2018). Shokrieh (Shokrieh, Nasir *et al*. 2012) presented a new model to calculate longitudinal strength of unidirectional composites exposed to sulfuric acid environment using the micromechanics theorem and emphasized on effect of thermal residual stresses. In most cases, the applications were limited to unidirectional multilayered materials. Afterward, a few researchers also used the micromechanical analysis for cross-ply laminates to study the residual thermal stress, crack inception and growth and viscoplastic and viscoelastic behaviors (Bigelow 1993, Xia, Chen *et al*. 2000, Chen, Xia *et al*. 2001, Ellyin, Xia *et al*. 2002, Zhang, Xia *et al*. 2005, Ahmadi 2017, Ebrahimi and Habibi 2018, Hamedi, Golestanian *et al*. 2018, Khodjet-Kesba, Benkhedda *et al*. 2018, Naghdinasab, Farrokhabadi *et al*. 2018). Xia (Xia, Zhang *et al*. 2003) analyzed unidirectional angle-ply laminates under multiaxial loading conditions using the finite element method in micromechanics and utilized periodic boundary conditions applicable only for the rhombohedral RVE models. He also showed that not only do the homogeneous boundary conditions have extra constraints but also that they violate the boundary traction continuity conditions. Xia (Xia, Zhou *et al*. 2006) proved the uniqueness of the solution of periodic boundary conditions problems using the displacement difference boundary condition in the displacement-based finite elements method. He proved that the solution does not depend on the choice of repeated unit cells (RUC), and using periodic boundary conditions guarantees the boundary traction continuity conditions. The combination of the homogenization theory with the finite element method is a very powerful technique, capable of analyzing complex microstructures with different shapes and directions and even random distribution in order to determine the effective mechanical properties of composite materials (Xia, Ju *et al*. 2007, Xu and Xu 2008). ABAQUS is a commercial software package used extensively in the analysis of RVEs (Lubineau and Ladeveze 2008, Yuan and Fish 2008). Wu (Wu, Owino *et al*. 2014) mentioned the complexity of applying periodic boundary conditions in finite elements software such as ABAQUS, and demonstrated the process of applying periodic boundary conditions via "input file" in a simple example. Also, Python code makes it possible to leverage the advanced finite element analysis of ABAQUS and enables the use of ABAQUS scripting interface. ASI is, in fact, an extension of the Python programming language used in modeling and extraction of results. Zuo (Zuo and Xie 2015) managed to use ASI in his work to optimize complex and 3D topologies.

In this paper, an RVE and its components (fiber and resin) have been modeled using ASI and the asymptotic homogenization theory. By applying periodic boundary conditions (PBCs), the mechanical properties of the composite material were determined using strain energy. The results were compared with those of the homogeneous boundary conditions (HBCs) method to illustrate the advantage of PBCs, especially in shear loading cases. Since in reality, resin exhibits a nonlinear behavior compared to fiber, the effects of this nonlinear behavior on the mechanical properties of the composite materials are considered in different fiber volume fractions using a USDFLD subroutine. This study, in contrast with the work of Xia (Xia, Zhang *et al*. 2003) is independent of the RVE geometry or the properties of its components. Thus, it is applicable to extract mechanical properties of complex structures with nonlinear component behavior, any arbitrary geometrical shape, and random distribution of the reinforcement.

2. Periodic boundary conditions

Composite materials can be considered a periodic array of RVEs. This is why periodic boundary conditions need to be applied to them. This means that the deformation of all RVEs is the same, there is no distance between two adjacent RVEs and that they don't overlap. The periodic boundary conditions are as follows (Suquet 1987)

$$u_i(x_1,x_2,x_3) = \bar{\varepsilon}_{ik} x_k + u_i^*(x_1,x_2,x_3) \tag{1}$$

where $\bar{\varepsilon}_{ik}$ is the average strain and $u_i^*(x_1,x_2,x_3)$ is a periodic function from one RVE to the next, which is essentially unknown and dependent on the general loading.

Due to the periodic placement of RVEs in a structure, two kinds of continuity must be satisfied in RVE boundaries: a) the displacements must be continuous and similar, such that no two adjacent RVEs will separate or overlap after deformation; and b) the traction distribution in opposite boundaries in an RVE must be the same. This will result in a continuous configuration. Displacement field assumption in the form of Eq. (1) can only be done according to the above considerations. Unfortunately, this equation cannot be directly applied to the boundaries due to the periodic part $u_i^*(x_1,x_2,x_3)$ is unknown. The boundary surfaces of an RVE must be assumed as parallel pairs where the displacement in both the opposing boundary surfaces can be written as follows

$$u_i^{j+} = \bar{\varepsilon}_{ik} x_k^{j+} + u_i^* \tag{2}$$

$$u_i^{j-} = \bar{\varepsilon}_{ik} x_k^{j-} + u_i^* \tag{3}$$

where the $j+$, $j-$ indices denote the jth pair of parallel opposing surfaces in an RVE. As stated before, the periodic part of Eq. (1), $u_i^*(x_1,x_2,x_3)$, is unknown but its value is the same for a pair of parallel surfaces. Therefore the difference between their displacements can be written as follows:

$$u_i^{j+} - u_i^{j-} = \bar{\varepsilon}_{ik}(x_k^{j+} - x_k^{j-}) = \bar{\varepsilon}_{ik}\Delta x_k^j \tag{4}$$

This eliminates the unknown periodic part of the displacement field. For each parallelepiped RVE model, the amount of Δx_k^j is constant, and, knowing the value of $\bar{\varepsilon}_{ik}$, the right-hand side of the equation will be constant. This transforms Eq. (4):

$$u_i^{j+}(x,y,z) - u_i^{j-}(x,y,z) = c_i^j, \quad (i,j = 1,2,3) \tag{5}$$

where the constants, c_2^2 and c_3^3 denote the average contraction and expansion of the RVE model due to normal traction components, while the other three pairs of constants, $c_1^2 = c_2^1$, $c_1^3 = c_3^1$ and $c_2^3 = c_3^2$ are related to shear deformation due to the shear components.

As it is evident from Eq. (5), this relation is written between node pairs on opposing boundary surfaces, and a plane may not remain planar after deformation. Also, Eq. (5) does not have the periodic part of the displacement field, making its utilization in the finite elements process as a constraint of the node displacement equation type, easier compared to Eq. (1). Eq. (5) is a special type of boundary condition of the displacement kind, which expresses the displacement difference between node pairs on opposing parallel surfaces, instead of the amount of displacement on boundaries. One may imagine that a boundary condition of the displacement difference type does not guarantee the traction continuity condition:

$$\sigma_n^{j+} - \sigma_n^{j-} = 0 \tag{6}$$

$$\tau_{nt}^{j+} - \tau_{nt}^{j-} = 0 \tag{7}$$

where σ_n and τ_{nt} denote the normal and shear stresses in opposing parallel surfaces.

Xia (Xia, Zhou *et al*. 2006) proved in his works that in displacement-based finite elements micromechanical analysis, using Eq. (5) guarantees the uniqueness of the solution, and Eqs. (6)-(7) will be automatically satisfied, thus there is no need to apply them in the analysis.

3. Homogenization

Homogenization is carried out to identify the behavior of the RVE in response to an applied mechanical loading and eventually, the estimation of mechanical properties. It is assumed that the average mechanical properties of the RVE is the same as those of composite laminates. The average stresses and strains in an RVE are defined as follows:

$$\bar{\sigma}_{ij} = \frac{1}{V_{RVE}}\int_v \sigma_{ij}\,dV = \frac{1}{V_{RVE}}\sum_{k=1}^{N}\sigma_{ij}^k V^k \tag{8}$$

$$\bar{\varepsilon}_{ij} = \frac{1}{V_{RVE}}\int_v \varepsilon_{ij}\,dV = \frac{1}{V_{RVE}}\sum_{k=1}^{N}\varepsilon_{ij}^k V^k \tag{9}$$

where V_{RVE} denotes the volume of RVE, σ_{ij}^k, ε_{ij}^k and V^k denote the stress, strain and volume of the kth element, respectively. $\bar{\sigma}_{ij}^k$ and $\bar{\varepsilon}_{ij}^k$ denote the average stress and strain.

The strain energy of the applied displacement under periodic conditions can be used to determine the homogenized module. If the strain is not zero, the strain energy due to displacement can be expressed as follows:

$$U = \frac{1}{2}\bar{\sigma}_{ij}\,\bar{\varepsilon}_{ij} V_{RVE} \tag{10}$$

where U denotes the total strain energy and $\bar{\varepsilon}_{ij}$ can be obtained via the applied displacement. $\bar{\sigma}_{ij}$ can be calculated using the total strain energy and the average strain from Eq. (10). This eliminates the need to use the general relations of average stress and strain, Eqs. (8)-(9).

The obtained strain energy from different boundary conditions must satisfy the following inequality if the average strain is the same for all boundary conditions:

$$U^T \le U^P \le U^D \tag{11}$$

where U^T, U^P and U^D denote the strain energy of homogeneous traction boundary conditions, periodic boundary conditions, and homogenous displacement boundary conditions, respectively. It is clear that using the homogenous displacement boundary conditions leads to an overestimation of effective mechanical properties while using the homogeneous traction boundary conditions results in an underestimation compared to ideal conditions. It is worth noting that using the homogenous displacement boundary conditions will not guarantee the continuity of traction at boundaries, also using the homogeneous traction boundary conditions will not ensure the continuity of displacement at boundaries.

The ratio of average stresses and strains computed as follow:

$$C_{ij} = \frac{\bar{\sigma}_{ij}}{\bar{\varepsilon}_{ij}} \tag{12}$$

where C_{ij} are the components of the stiffness matrix.

In the case of pure shear deformation, the following relation holds:

$$\gamma_{ij} = \varepsilon_{ij} + \varepsilon_{ij} = 2\varepsilon_{ij} \tag{13}$$

where γ_{ij} denotes the engineering shear strain.

If the RVE is assumed to be unidirectional and orthotropic with a linear behavior in the elastic zone, the constitutive equation for a 3D RVE will be:

$$\begin{Bmatrix} \bar{\sigma}_{11} \\ \bar{\sigma}_{22} \\ \bar{\sigma}_{33} \\ \bar{\sigma}_{12} \\ \bar{\sigma}_{13} \\ \bar{\sigma}_{23} \end{Bmatrix} = \begin{bmatrix} C_{11} & C_{12} & C_{13} & 0 & 0 & 0 \\ C_{12} & C_{22} & C_{23} & 0 & 0 & 0 \\ C_{13} & C_{23} & C_{33} & 0 & 0 & 0 \\ 0 & 0 & 0 & C_{44} & 0 & 0 \\ 0 & 0 & 0 & 0 & C_{55} & 0 \\ 0 & 0 & 0 & 0 & 0 & C_{66} \end{bmatrix} \begin{Bmatrix} \bar{\varepsilon}_{11} \\ \bar{\varepsilon}_{22} \\ \bar{\varepsilon}_{33} \\ \bar{\varepsilon}_{12} \\ \bar{\varepsilon}_{13} \\ \bar{\varepsilon}_{23} \end{Bmatrix} \tag{14}$$

Considering Eqs. (10), (12) and (14), the relation between strain energy and average strain is obtained as:

$$U = \frac{1}{2}\left[\bar{\varepsilon}\right]^T \left[\bar{\varepsilon}\right] V_{RVE} \tag{15}$$

$$\begin{aligned} \frac{U}{V_{RVE}} &= \frac{1}{2}C_{11}\bar{\varepsilon}_{11}^{2} + C_{12}\bar{\varepsilon}_{11}\bar{\varepsilon}_{22} + C_{13}\bar{\varepsilon}_{11}\bar{\varepsilon}_{33} \\ &+ \frac{1}{2}C_{22}\bar{\varepsilon}_{22}^{2} + C_{23}\bar{\varepsilon}_{22}\bar{\varepsilon}_{33} + \frac{1}{2}C_{33}\bar{\varepsilon}_{33}^{2} + \frac{1}{2}C_{44}\bar{\varepsilon}_{12}^{2} \\ &+ \frac{1}{2}C_{55}\bar{\varepsilon}_{13}^{2} \frac{1}{2}C_{66}\bar{\varepsilon}_{23}^{2} \end{aligned} \tag{16}$$

With the average strain components, strain energy and RVE volume, the stiffness matrix components can be obtained from Eq. (16).

To determine the compliance matrix, the inverse of the stiffness matrix can be used:

$$[S] = [C]^{-1} \tag{17}$$

Knowing the components of the compliance matrix, the effective mechanical properties of the RVE can be calculated:

$$\begin{aligned} E_1 &= \frac{1}{S_{11}}, \nu_{12} = -\frac{S_{12}}{S_{11}}, G_{12} = \frac{1}{S_{44}} \\ E_2 &= \frac{1}{S_{22}}, \nu_{13} = -\frac{S_{13}}{S_{11}}, G_{13} = \frac{1}{S_{55}} \\ E_3 &= \frac{1}{S_{33}}, \nu_{23} = -\frac{S_{23}}{S_{33}}, G_{23} = \frac{1}{S_{66}} \end{aligned} \tag{18}$$

where E_i, G_{ij}, v_{ij} and denote the modulus of S_{ij}, elasticity, shear modulus, Poisson's ratio and components of the flexibility matrix, respectively.

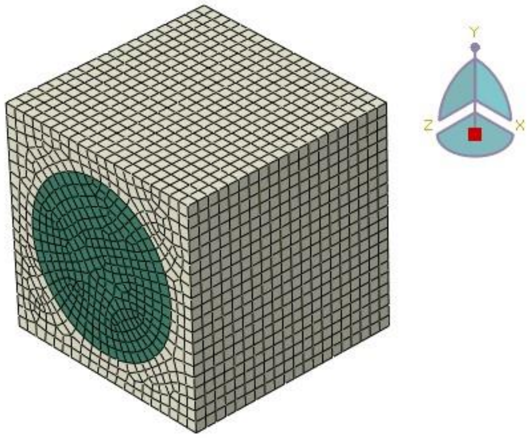

Fig. 1 Meshed unidirectional RVE model with unit dimensions

4. Finite element modeling

The RVE shown in Fig. 1, has been modeled in three dimensions, with unit dimensions ($\Delta x = \Delta y = \Delta z = 1$), using 8 node hexahedral C3D8R elements. 11060 elements have been used to create a unidirectional RVE.

4.1 Constraint Equations in ABAQUS

Periodic boundary conditions are applied as linear constraints in ABAQUS. A large number of points can be constrained using a linear combination of nodal variables such as the displacement of different nodes. The sum of the nodal variables multiplied by their coefficients must be zero. Therefore, the linear homogenous equation in its general form is defined as follows (Wu, Owino *et al.* 2014)

$$A_1 u_i^P + A_2 u_j^Q + \ldots + A_N u_k^R = 0 \tag{19}$$

where P, Q and R represent nodes and i , j and k denote the directions of freedom. A_1, A_2 and A_N denote constant coefficients underlining the share of each nodal variable in the equation. In ABAQUS the keyword *EQUATION is used to create linear constraints for N nodes.

4.2 Dummy node

To apply periodic boundary conditions using the constraint equations mentioned above, the concept of dummy nodes is introduced in ABAQUS. By substituting a non-zero value instead of zero in the right-hand side of Eq. (19), the following equation is obtained:

$$A_1 u_i^P + A_2 u_j^Q + \ldots + A_N u_k^R = u \tag{20}$$

where u is a determined value such as strain or displacement.

This determined value of strain or displacement is applied to the dummy node which is not connected to any part of the created model. To this end, a reference point with arbitrary coordinates is created to define this dummy node. The value u is applied to this reference point as a boundary condition in a fixed direction.

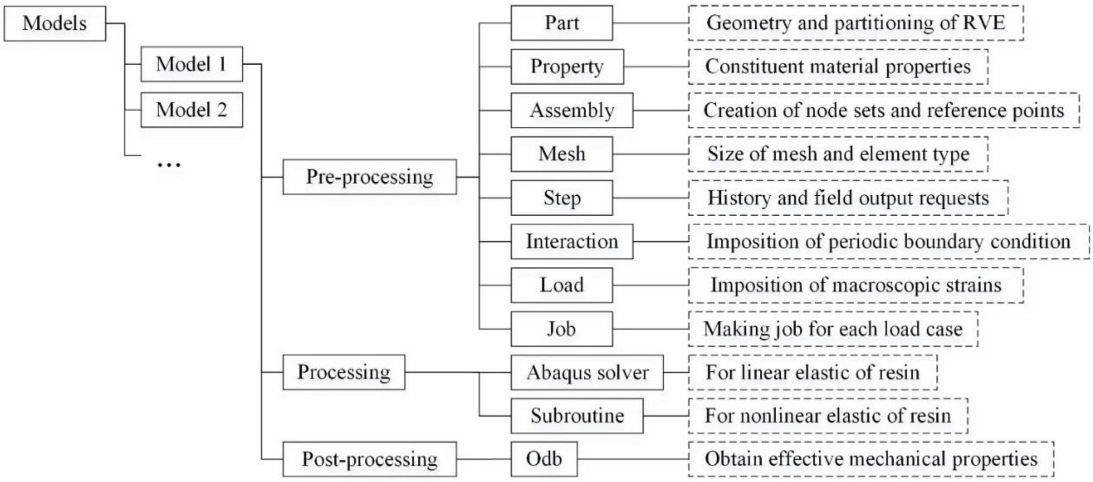

Fig. 2 Python scripting flowchart for RVE modeling to obtain effective mechanical properties

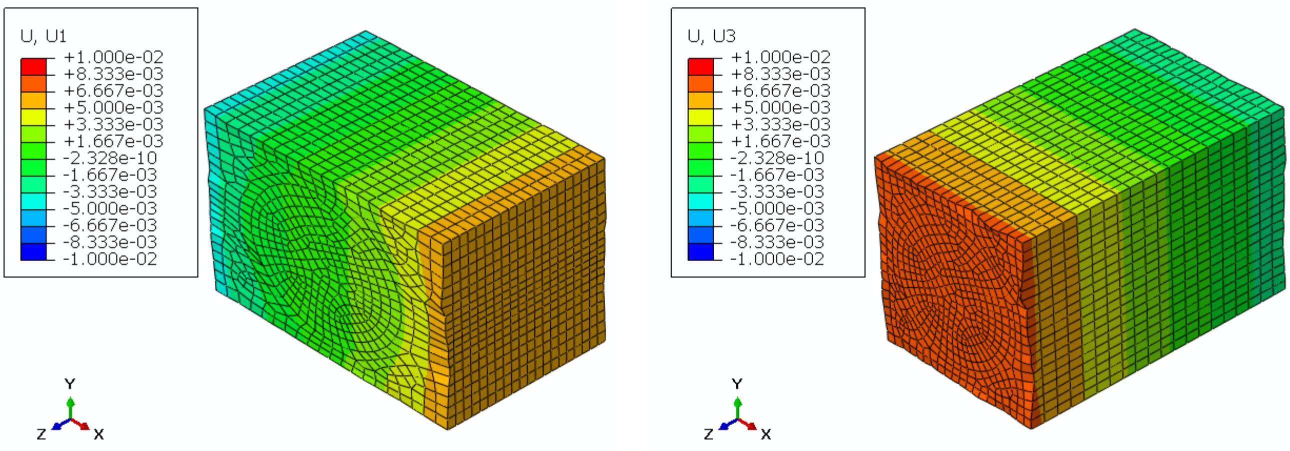

(a) normal strain $\varepsilon_{11} = 0.01$ (b) normal strain $\varepsilon_{33} = 0.01$

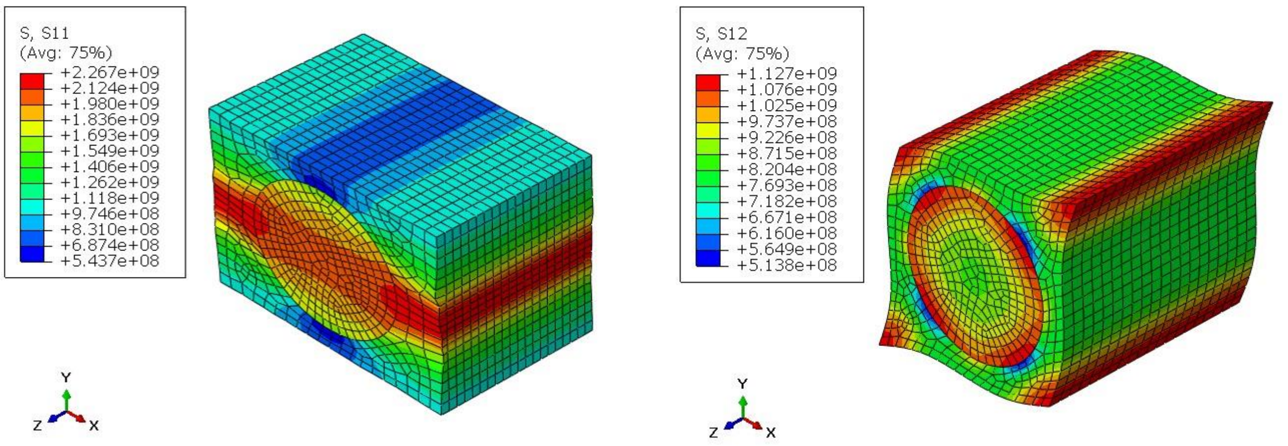

(c) normal strain $\varepsilon_{11} = 0.01$ (d) shear strain $\varepsilon_{12} = 0.01$

Fig. 3 The displacement and stress field of different loading stages

4.3 Meshing

In finite element analysis, appropriate meshing is required to obtain meaningful results. In the RVE modeled in this study, the constraints on meshing are more severe. To apply periodic boundary conditions on the RVE, both the opposing parallel surfaces must have the same meshing pattern, so that the node pairs on the opposing faces will have the same in-plane coordinates, and it will be possible to apply the displacement constraint equations in the three *x*, *y* and *z* direction on the RVE. This is only possible by copying the mesh pattern of a surface on its opposing surface.

Table 1 Required equations to apply the periodic boundary conditions in node pairs

Face Nodes	Edge Nodes	Vertex Nodes
$u_i^{FGCB} - u_i^{EHDA} - \Delta x\, \varepsilon_{i1} = 0$	$u_i^{GF} - u_i^{DA} - \Delta x\, \varepsilon_{i1} - \Delta y\, \varepsilon_{i2} = 0$	$u_i^{G} - u_i^{A} - \Delta x\, \varepsilon_{i1} - \Delta y\, \varepsilon_{i2} - \Delta z\, \varepsilon_{i3} = 0$
$u_i^{FEHG} - u_i^{BADC} - \Delta y\, \varepsilon_{i2} = 0$	$u_i^{CB} - u_i^{HE} - \Delta x\, \varepsilon_{i1} + \Delta y\, \varepsilon_{i2} = 0$	$u_i^{F} - u_i^{D} - \Delta x\, \varepsilon_{i1} - \Delta y\, \varepsilon_{i2} + \Delta z\, \varepsilon_{i3} = 0$
$u_i^{GHDC} - u_i^{FEAB} - \Delta z\, \varepsilon_{i3} = 0$	$u_i^{GC} - u_i^{EA} - \Delta x\, \varepsilon_{i1} - \Delta z\, \varepsilon_{i3} = 0$	$u_i^{H} - u_i^{B} + \Delta x\, \varepsilon_{i1} - \Delta y\, \varepsilon_{i2} - \Delta z\, \varepsilon_{i3} = 0$
	$u_i^{FB} - u_i^{HD} - \Delta x\, \varepsilon_{i1} + \Delta z\, \varepsilon_{i3} = 0$	$u_i^{C} - u_i^{E} - \Delta x\, \varepsilon_{i1} + \Delta y\, \varepsilon_{i2} - \Delta z\, \varepsilon_{i3} = 0$
	$u_i^{GH} - u_i^{BA} - \Delta y\, \varepsilon_{i2} - \Delta z\, \varepsilon_{i3} = 0$	
	$u_i^{FE} - u_i^{CD} - \Delta y\, \varepsilon_{i2} + \Delta z\, \varepsilon_{i3} = 0$	

Since a constraint equation is needed for every node pairs in each of the x, y and z directions, there will be so many of these constraint equations that applying them without an automatic procedure (Python script) will be almost impossible.

4.4 Loading

For loading, six macroscopic strains ε_{11}, ε_{22}, ε_{33}, ε_{12}, ε_{13} and ε_{23} are applied individually on the RVE to find the six components of the stiffness matrix, C_{11}, C_{22}, C_{33}, C_{44}, C_{55} and C_{66}. Mixed loading can also be used to determine the C_{12}, C_{13} and C_{23} components of the stiffness matrix. In other words, loading must be applied in nine stages in the RVE model to obtain the nine components of the stiffness matrix. Fig. 3 depicts the different stages of normal, and shear loading applied to the RVE.

4.5 Applying the periodic boundary conditions

The procedure for applying periodic boundary conditions on the RVE model is detailed below (Shahzamanian, Tadepalli *et al*. 2014):

- First, the nodes must be divided into three groups: face nodes, edge nodes and vertex nodes, in a way that each node is only in one group, and the groups have no common members so that no over-constraint happens.
- Using the keyword *EQUATION to create the constraint equations between the node pairs on opposing faces. These equations are detailed in Table 1 separately for each node group in Fig. 4.
- Creating as many dummy nodes as the equations in Table 1 and assigning each node to an equation.
- Applying the specified loadings on the dummy nodes, which are outside the RVE model zone

The general procedure for Python scripting from the beginning of RVE modeling up until extracting the results is shown in Fig. 2.

5. Results

One simple way to find out whether the applied periodic boundary conditions are working correctly or not, is to subject a model with isotropic and simple geometry to the intended procedure for applying the periodic boundary conditions. If the procedure is indeed correct, similar strains and stresses must be induced across the entirety of the isotropic model, which are equal to the average strain and stress.

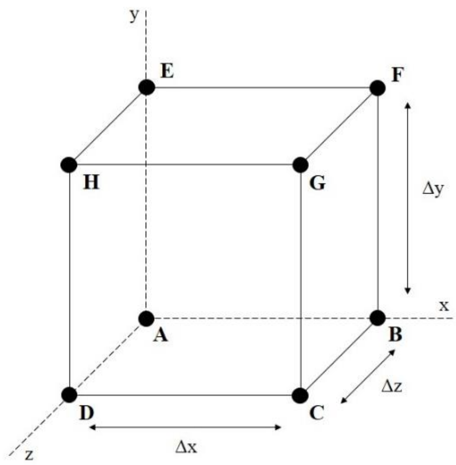

Fig. 4 Naming the vertices, edges, and faces of the RVE for applying the periodic boundary conditions

Table 2 The mechanical properties of fiber and resin

Material	Modulus of Elasticity (GPa)	Poisson’s Ratio
Boron	379.3	0.1
Aluminum	68.3	0.3
E-glass	72.5	0.22
Epoxy	3.54	0.38

5.1 The linear elastic behavior of resin

In this part, the modeled RVE is comprised of Boron fiber and Aluminum matrix, as a unidirectional laminate composite, with the mechanical properties presented in Table 2, and a fiber volume fraction of 47%, which are individually isotropic but have different mechanical properties.

It is worth noting that in materials with an overall orthotropic behavior, according to Eq. (14), there are nine independent components in the three-dimensional case, but based on Fig. 1, the modeled unidirectional RVE has similar behavior in the x and y directions, and is thus a transversely isotropic material. Therefore the mechanical properties of the two x and y directions can be written as: $E_1=E_2$, $\nu_{13}=\nu_{23}$. By comparison of the results of this study and those of past analytical and experimental studies, listed in Table 3, the validity of the present procedure is proved. Using homogenous displacement boundary conditions, plane-

Table 3 The results for the mechanical properties of the multi-layered composite of Boron / Aluminum

Mechanical Properties	Present		Numerical (Periodic BC) (Xia, Zhang *et al.* 2003)	Numerical (Symmetric BC) (Sun and Vaidya 1996)	Analytical (Elastic-Plastic) (Sun and Chen 1991)	Analytical (Micromechanics Equations) (Chamis 1983)	Analytical (Energy variation) (Hashin and Rosen 1964)	Experimental (Kenaga, Doyle *et al.* 1987)
	PBC	HBC						
$E_3(GPa)$	214.9	215	214	215	214	214	215	216
$E_2(GPa)$	143.6	145	143	144	135	156	135.2	140
$G_{23}(GPa)$	54.2	71.9	54.2	57.2	51.1	62.6	53.9	52
$G_{12}(GPa)$	45.7	51.5	45.7	45.9	-	43.6	52.3	-
ν_{23}	0.195	0.195	0.195	0.19	0.19	0.20	0.195	0.29
ν_{12}	0.255	0.249	0.253	0.29	-	0.31	0.295	-

remains-plane, is acceptable when normal traction is applied to the boundaries, while in the case of shear loading, results are an overestimation of the effective mechanical properties due to over-constrained boundary conditions. To apply the homogenous displacement boundary conditions, the relations suggested by Aliabadi (Aliabadi 2015) have been utilized, which leads to the overestimation of shear moduli according to the data in Table 3. Compared to the periodic boundary conditions case, each of the shear moduli G_{23} and G_{12} increased by 33% and 13%, respectively, with the application of the homogeneous boundary conditions. Therefore, using the homogenous displacement boundary conditions for an RVE subjected to shear loading is not appropriate.

5.2 The nonlinear elastic behavior of resin

In reality, resin exhibits a nonlinear behavior in the elastic zone, which causes the unidirectional multilayered composite to have a nonlinear shear stress-strain relation. In this section, the effects of this nonlinear behavior on the shear stress-strain diagram of the unidirectional composites laminate, considering the fiber volume fraction, has been addressed. The nonlinear constitutive equation of resin under tension has been assumed to be an 3^{rd} order polynomial:

$$\varepsilon_{ij} = \frac{\sigma_{ij}}{E_{ij}} + \alpha\sigma_{ij}^3 \qquad (i, j = 1, 2, 3) \tag{21}$$

where α denotes the nonlinear coefficient of resin.

To use the nonlinear equation in the computer code, the instantaneous (tangential) elasticity modulus must be calculated. Differentiating Eq. (21) concerning tensile stress yields the instantaneous (tangential) modulus:

$$\frac{\partial\sigma_{ij}}{\partial\varepsilon_{ij}} = \frac{1}{\dfrac{1}{E_{ij}} + 3\alpha\sigma_{ij}^2} \tag{22}$$

To obtain the nonlinear equation between normal stress and strain, the relation of stress and strain must be described in a different form. In other words, at the end of an increment, stress must be a linear function of strain. The simplest way to achieve this is by linearizing the nonlinear terms as (Simulia 2013):

$$\varepsilon_{ij}^{(k+1)} = \left(E_{ij}^{-1} + \alpha\left(\sigma_{ij}^{(k)}\right)^2\right)\sigma_{ij}^{(k+1)} \tag{23}$$

where k denotes the increment index.

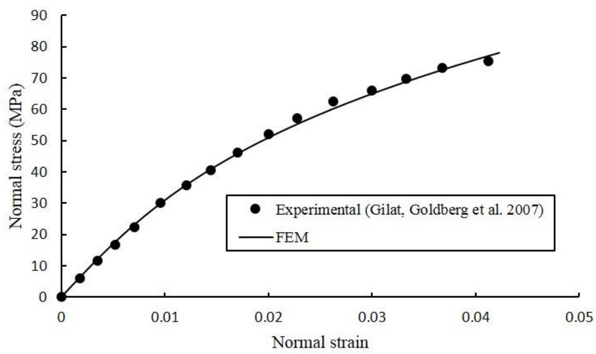

Fig. 5 The tensile stress-strain diagram of the epoxy resin

Since using Eq. (23) results in instability with higher levels of strain, Eq. (24) can be used, which is an optimized algorithm obtained from the previous relation. Finally, this relation is written in the form of Eq. (26) as a function of the damage parameter, then it is implemented inside the USDFLD subroutine, and the value of the damage parameter is thus directly assigned to the field variables required for defining the elastic properties.

$$\sigma_{ij}^{(k+1)} = \frac{1 + \dfrac{2\alpha(\sigma_{ij}^{(k)})^3}{\varepsilon_{ij}^{(k)}}}{1 + 3\alpha E_{ij}(\sigma_{ij}^{(k)})^2} E_{ij}\varepsilon_{ij}^{(k+1)} \tag{24}$$

$$\sigma_{ij}^{(k+1)} = (1-d)E_{ij}\varepsilon_{ij}^{(k+1)} \tag{25}$$

$$d = \frac{3\alpha E_{ij}(\sigma_{ij}^{(k)})^2 - \dfrac{2\alpha(\sigma_{ij}^{(k)})^3}{\varepsilon_{ij}^{(k)}}}{1 + 3\alpha E_{ij}(\sigma_{ij}^{(k)})^2} \tag{26}$$

Fig. 5 depicts the normal stress-strain diagram obtained from the epoxy resin tension test (Gilat, Goldberg *et al.* 2007), the properties of which are listed in Table 2. The.

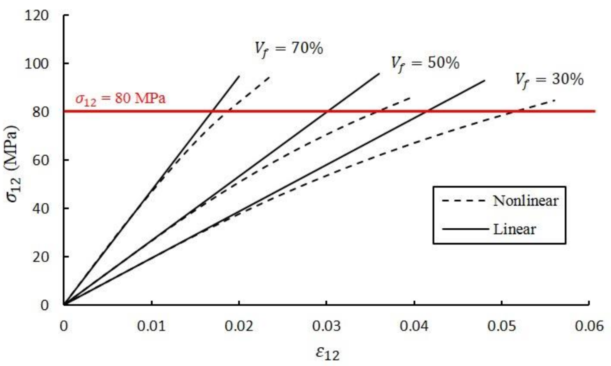

Fig. 6 The linear and nonlinear diagram of $\sigma_{12}-\varepsilon_{12}$ in different fiber volume fractions

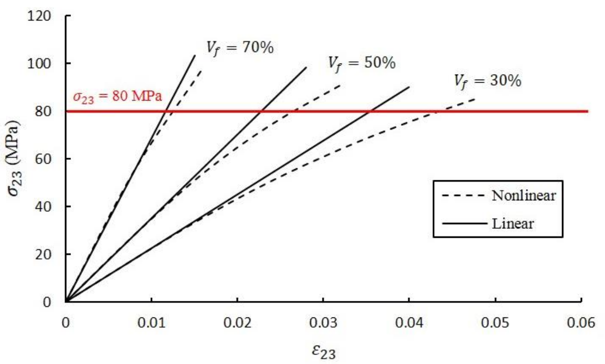

Fig. 7 The linear and nonlinear diagram of $\sigma_{23}-\varepsilon_{23}$ in different fiber volume fractions

diagram is resulting from Eq. (21) is also presented in Fig 5, exhibiting a good agreement with the experimental curve. The value α is obtained by curve fitting on the experimental curve using Eq. (21) as $4.267\times10^{-26} Pa^{-3}$. This is substituted in Eq. (26).

In this section, the modeled RVE, as a unidirectional composite laminate, is formed from glass fiber and epoxy resin with the mechanical properties listed in Table 2 with fiber volume fractions of 30%, 50% and 70%. Figs. 6 and 7 depict the linear and nonlinear diagrams of $\sigma_{12}-\varepsilon_{12}$ and $\sigma_{23}-\varepsilon_{23}$ curves, respectively, in the elastic zone. The effect of fiber volume fraction on these curves is visible. Under constant stress, the lower the fiber volume fraction, the linear and nonlinear curves are pushed farther and farther apart, while in high fiber volume fractions, the nonlinearity of the shear stress-strain curve decreases.

To compare the degree of nonlinearity of the shear behavior in composite laminates, the amount of drop in the shear moduli G_{12} and G_{23}under arbitrary constant stress as 80 MPa has been reported. In Fig. 6 the shear modulus G_{12} G_{12} equals 1.94, 2.66 and 4.74 GPa in 30%, 50% and 70% fiber volume fractions, respectively, which is decreased in the nonlinear diagram by 47%, 41%, and 31%, respectively. Fig. 7 depicts the shear modulus G_{23} having the value of 2.25, 3.51 and 6.89 GPa with 30%, 50% and 70% fiber volume fractions, respectively, while it experiences a 45%, 39% and 27% drop under a constant 80 MPa stress, due to nonlinear shear behavior.

6. Conclusion

Applying periodic boundary conditions guarantees the continuity of traction, as well as the continuity of displacement at the boundaries of the RVE and any periodic structure made of composite laminates under multiaxial loading. It was shown that using homogenous boundary conditions, plane-remains-plane, under shear loading is not appropriate and leads to an overestimation of the effective mechanical properties of the RVE. The results indicate that applying homogenous boundary conditions results in a 33% and 13% increase in the shear moduli G_{23} and G_{12}, respectively.

The Python code developed in this research can be used to extract the mechanical properties of complex structures with random shape, direction and distribution of the reinforcing part.

This solution does not depend on the properties of the RVE components, which is the reason it can be used for nonlinear analyses. The nonlinear behavior of resin in the elastic zone was examined, and its effects on the shear stress-strain curve of the unidirectional composite laminate were studied. Results indicate that at arbitrary constant stress as 80 MPa in-plane shear modulus, G_{12}, experienced a 47%, 41% and 31% reduction at the fiber volume fraction of 30%, 50% and 70%, compared to the linear assumption.

References

Aboudi, J. (1990), "Micromechanical prediction of initial and subsequent yield surfaces of metal matrix composites", *J. Plasticity*, **6**(4), 471-484. https://doi.org/10.1016/0749-6419(90)90014-6.

Aboudi, J. (2013), *Mechanics of Composite Materials: A Unified Micromechanical Approach*, Elsevier, The Netherlands.

Adams, D.F. and Crane, D.A. (1984), "Finite element micromechanical analysis of a unidirectional composite including longitudinal shear loading", *Comput. Struct.*, **18**(6), 1153-1165. https://doi.org/10.1016/0045-7949(84)90160-3.

Ahmadi, I. (2017), "Micromechanical failure analysis of composite materials subjected to biaxial and off-axis loading", *Struct. Eng. Mech.*, **62**(1), 43-54. https://doi.org/10.12989/sem.2017.62.1.043

Aliabadi, M.H. (2015), *Woven Composites*, Imperial College Press, London, United Kingdom.

Allen, D.H. and Boyd, J.G. (1993), "Convergence rates for computational predictions of stiffness loss in metal matrix composites", *Composite Materials and Structures*, **AMD 179/AD 37**, ASME, New York, USA. 31-45.

Bakhvalov, N.S. and Panasenko, G.P. (1984), *Homogenization in Periodic Media, Mathematical Problems of the Mechanics of Composite Materials*, Nauka, Moscow, Russia.

Belkacem, A., Tahar, H.D., Abderrezak, R., Amine, B.M., Mohamed, Z. and Boussad, A. (2018), "Mechanical buckling analysis of hybrid laminated composite plates under different boundary conditions", *Struct. Eng. Mech.*, **66**(6), 761-769. https://doi.org/10.12989/sem.2018.66.6.761.

Bensoussan, A., Lions, J.L. and Papanicolaou, G. (2011), *Asymptotic Analysis for Periodic Structures*, American Mathematical Society, Providence, Rhode Island, USA.

Bigelow, C.A. (1993), "Thermal residual stresses in a silicon-carbide/titanium [0/90] laminate", *J. Compos. Technol. Res.*, **15**(4), 304-310. https://doi.org/10.1520/CTR10383J.

Bonora, N., Costanzi, M., Newaz, G. and Marchetti, M. (1994), "Microdamage effects on the overall response of long fibre/metal-matrix composites", *Compos.,* **25**(7), 575-582. https://doi.org/10.1016/0010-4361(94)90187-2.

Chamis, C.C. (1983), "Simplified composite micromechanics for hygral, thermal and mechanical properties", *SAMPE Quarterly*, 14-23. https://ntrs.nasa.gov/search.jsp?R=19830011546.

Chen, Y., Xia, Z. and Ellyin, F. (2001), "Evolution of Residual Stresses Induced during Curing Processing Using a Viscoelastic Micromechanical Model", *J. Compos. Mater.*, **35**(6), 522-542. https://doi.org/10.1177%2F002199801772662145.

Chu, X., Yu, C., Xiu, C. and Xu, Y. (2015), "Two scale modeling of behaviors of granular structure: size effects and displacement fluctuations of discrete particle assembly", *Struct. Eng. Mech.*, **55**(2), 315-334. https://doi.org/10.12989/sem.2015.55.2.315.

Ebrahimi, F. and Habibi, S. (2018), "Thermal effects on nonlinear dynamic characteristics of polymer-CNT-fiber multiscale nanocomposite structures", *Struct. Eng. Mech.*, **67**(4), 403-415. https://doi.org/10.12989/sem.2018.67.4.403.

Ellyin, F., Xia, Z. and Chen, Y. (2002), "Viscoelastic micromechanical modeling of free edge and time effects in glass fiber/epoxy cross-ply laminates", *Composites Part A Appl. Sci. Manufact.*, **33**(3), 399-409. https://doi.org/10.1016/S1359-835X(01)00112-9.

Gilat, A., Goldberg, R.K. and Roberts, G.D. (2007), "Strain Rate Sensitivity of Epoxy Resin in Tensile and Shear Loading", *J. Aerosp. Eng.*, **20**(2), 75-89. https://doi.org/10.1061/(ASCE)0893-1321(2007)20:2(75).

Guedes, M. and Kikuchi, N. (1990), "Preprocessing and postprocessing for materials based on the homogenization method with adaptive finite element methods", *Comput. Methods Appl. Mech. Eng.*, **83**, 143-198. https://doi.org/10.1016/0045-7825(90)90148-F.

Hamedi, M., Golestanian, H., Tadi Beni, Y. and Alasvand Zarasvand, K. (2018), "Evaluation of fracture energy for nanocomposites reinforced with carbon nanotubes using numerical and micromechanical methods", *Mech. Adv. Mater. Struct.*, 1-9. https://doi.org/10.1080/15376494.2018.1432787.

Hashin, Z. and Rosen, B.W. (1964), "The Elastic Moduli of Fiber-Reinforced Materials", *J. Appl. Mech.*, **31**, 223-232.

Hashin, Z. and Shtrikman, S. (1963), "A variational approach to the theory of the elastic behaviour of multiphase materials", *J. Mech. Phys. Solids*, **11**, 127-140. https://doi.org/10.1016/0022-5096(63)90060-7.

Hollister, S.J. and Kikuchi, N. (1992), "A comparison of homogenization and standard mechanics analyses for periodic porous composites", *Comput. Mech.*, **10**(2), 73-95. https://doi.org/10.1007/BF00369853.

Hori, M. and Nemat-Nasser, S. (1999), "On two micromechanics theories for determining micro–macro relations in heterogeneous solids", *Mech. Mater.*, **31**(10), 667-682. https://doi.org/10.1016/S0167-6636(99)00020-4.

Kenaga, D., Doyle, J.F. and Sun, C.T. (1987), "The characterization of boron/aluminum composite in the nonlinear range as an orthotropic elastic-plastic material", *J. Compos. Mater.*, **21**(6), 516-531. https://doi.org/10.1177/002199838702100603.

Khodjet-Kesba, M., Benkhedda, A., Adda Bedia, E. and Boukert, B. (2018), "On transverse matrix cracking in composite laminates loaded in flexure under transient hygrothermal conditions", *Struct. Eng. Mech.*, **67**(2), 165-173. https://doi.org/10.12989/sem.2018.67.2.165.

Liao, B., Tan, H., Zhou, J. and Jia, L. (2018), "Multi-scale modelling of dynamic progressive failure in composite laminates subjected to low velocity impact", *Thin-Walled Struct.*, **131**, 695-707. https://doi.org/10.1016/j.tws.2018.07.047.

Lubineau, G. and Ladeveze, P. (2008), "Construction of a micromechanics-based intralaminar mesomodel, and illustrations in ABAQUS/Standard", *Comput. Mater. Sci.*, **43**(1), 137-145. https://doi.org/10.1016/j.commatsci.2007.07.050.

Ma, J., Wriggers, P. and Li, L. (2016), "Homogenized thermal properties of 3D composites with full uncertainty in the microstructure", *Struct. Eng. Mech.*, **57**(2), 369-387. https://doi.org/10.12989/sem.2016.57.2.369.

Moorthy, S. and Ghosh, S. (1998), "Particle cracking in discretely reinforced materials with the voronoi cell finite element model", *J. Plasticity*, **14**(8), 805-827. https://doi.org/10.1016/S0749-6419(98)00024-2.

Naghdinasab, M., Farrokhabadi, A. and Madadi, H. (2018), "A numerical method to evaluate the material properties degradation in composite RVEs due to fiber-matrix debonding and induced matrix cracking", *Finite Elements Analysis Design*, **146**, 84-95. https://doi.org/10.1016/j.finel.2018.04.008.

Needleman, A. and Tvergaard, V. (1993), "Comparison of Crystal Plasticity and Isotropic Hardening Predictions for Metal-Matrix Composites", *J. Appl. Mech.*, **60**, 70-76.

Nemat-Nasser, S. and Hori, M. (2013), *Micromechanics: Overall Properties of Heterogeneous Materials*, Elsevier, The Netherlands.

Pindera, M.J. and Aboudi, J. (1988), "Micromechanical analysis of yielding of metal matrix composites", *J. Plasticity*, **4**(3), 195-214. https://doi.org/10.1016/0749-6419(88)90010-1.

Raghavan, P., Moorthy, S., Ghosh, S. and Pagano, N.J. (2001), "Revisiting the composite laminate problem with an adaptive multi-level computational model", *Compos. Sci. Technol.,* **61**, 1017-1040. https://doi.org/10.1016/S0266-3538(00)00230-X.

Riley, M.B. and Whitney, J.M. (1966), "Elastic properties of fiber reinforced composite materials", *AIAA J.*, **4**(9), 1537-1542. https://doi.org/10.2514/3.3732.

Sánchez-Palencia, E. (1980), *Non-homogeneous Media and Vibration Theory*, *Lecture Notes in Physics Series Volume 127*, Springer, Berlin, Germany.

Shahzamanian, M.M., Tadepalli, T., Rajendran, A.M., Hodo, W.D., Mohan, R., Valisetty, R., Chung, P.W. and Ramsey, J.J. (2014), "Representative volume element based modeling of cementitious materials", *J. Eng. Mater. Technol.*, **136**(1), https://doi.org/10.1115/1.4025916.

Shokrieh, M., Nasir, V. and Karimipour, H. (2012), "A micromechanical study on longitudinal strength of fibrous composites exposed to acidic environment", *Mater. Design*, **35**, 394-403. https://doi.org/10.1016/j.matdes.2011.08.044.

Simulia, A.V. (2013), "6.13 Documentation", Dassault System, Vélizy-Villacoublay, France.

Sun, C.T. and Chen, J.L. (1991), "A micromechanical model for plastic behavior of fibrous composites", *Compos. Sci. Technol.*, **40**(2), 115-129. https://doi.org/10.1016/0266-3538(91)90092-4.

Sun, C.T. and Vaidya, R.S. (1996), "Prediction of composite properties from a representative volume element", *Compos. Sci. Technol.*, **56**, 171-179. https://doi.org/10.1016/0266-3538(95)00141-7.

Suquet, P. (1987), *Elements of Homogenization Theory for Inelastic Solid Mechanics, Homogenization Techniques for Composite Media*, Springer-Verlag, Berlin, Germany.

Tchalla, A., Belouettar, S., Makradi, A. and Zahrouni, H. (2013), "An ABAQUS toolbox for multiscale finite element computation", *Compos. Part B Eng.*, **52**, 323-333. https://doi.org/10.1016/j.compositesb.2013.04.028.

Wu, W., Owino, J., Al-Ostaz, A. and Cai, L. (2014), "Applying periodic boundary conditions in finite element analysis", *Simulia Community Conference*, 707-719.

Xia, Z., Chen, Y. and Ellyin, F. (2000), "A meso/micro-mechanical model for damage progression in glass-fiber/epoxy cross-ply laminates by finite-element analysis", *Compos. Sci. Technol.*, **60**, 1171-1179. https://doi.org/10.1016/S0266-3538(00)00022-1.

Xia, Z., Ju, F. and Sasaki, K. (2007), "A general finite element analysis method for balloon expandable stents based on repeated unit cell (RUC) model", *Finite Elements Anal. Design*, **43**(8), 649-658. https://doi.org/10.1016/j.finel.2007.01.001.

Xia, Z., Zhang, Y. and Ellyin, F. (2003), "A unified periodical boundary conditions for representative volume elements of composites and applications", *J. Solids Struct.*, **40**(8), 1907-1921. https://doi.org/10.1016/S0020-7683(03)00024-6.

Xia, Z., Zhou, C., Yong, Q. and Wang, X. (2006), "On selection of repeated unit cell model and application of unified periodic boundary conditions in micro-mechanical analysis of composites", *J. Solids Struct.*, **43**(2), 266-278. https://doi.org/10.1016/j.ijsolstr.2005.03.055.

Xu, K. and Xu, X.W. (2008), "Finite element analysis of mechanical properties of 3D five-directional braided composites", *Mater. Sci. Eng. A*, **487**(1-2), 499-509. https://doi.org/10.1016/j.msea.2007.10.030.

Yahia, S.A., Amar, L.H.H., Belabed, Z. and Tounsi, A. (2018), "Effect of homogenization models on stress analysis of functionally graded plates", *Struct. Eng. Mech.*, **67**(5), 527-544. https://doi.org/10.12989/sem.2018.67.5.527.

Yuan, Z. and Fish, J. (2008), "Toward realization of computational homogenization in practice", *J. Numerical Methods Eng.*, **73**(3), 361-380. https://doi.org/10.1002/nme.2074.

Zhang, Y., Xia, Z. and Ellyin, F. (2005), "Nonlinear viscoelastic micromechanical analysis of fibre-reinforced polymer laminates with damage evolution", *J. Solids Struct.*, **42**(2), 591-604. https://doi.org/10.1016/j.ijsolstr.2004.06.021.

Zuo, Z.H. and Xie, Y.M. (2015), "A simple and compact Python code for complex 3D topology optimization", *Adv. Eng. Software*, **85**, 1-11. https://doi.org/10.1016/j.advengsoft.2015.02.006.

CC